NASA DEVELOP National Program
California – JPL

Fall 2022

Western Tennessee Water Resources

Leveraging High Resolution Remotely Sensed Data to Assess Water Availability and Vulnerability in the Memphis Aquifer Area in West Tennessee

DEVELOP Technical Report

November 10th, 2022

Lauren Webster (Project Lead)
Elena Pilch
Katera Lee
Michael Pazmino

Advisors:
Madeleine Pascolini-Campbell, NASA Jet Propulsion Laboratory, California Institute of Technology
Kerry Cawse-Nicholson, NASA Jet Propulsion Laboratory, California Institute of Technology
Benjamin Holt, NASA Jet Propulsion Laboratory, California Institute of Technology

Previous Contributors:
Lauren Mahoney
Brenna Hatch
Claire Villanueva-Weeks
Lauren Webster

Fellow:
Kathleen Lange (California – JPL)

1. Abstract

The Memphis Aquifer (MA) is located in the Mississippi Embayment that extends 250,000 square kilometers across eight states. Fayette and Haywood counties in West Tennessee are situated within the recharge zone of the MA and include the forthcoming Ford "mega campus" named Blue Oval City (BOC), which will consist of a vehicle-production facility and battery assembly division. Increased water demand and land cover change resulting from urban development, such as BOC in the MA's narrow recharge zone, threaten the aquifer's groundwater storage and recharge rate. Groundwater recharge factors that influence the narrow recharge zone of the MA include precipitation, evapotranspiration, runoff, and land cover type. In partnership with Protect Our Aquifer (POA) and the Center for Applied Earth Science and Engineering Research (CAESAR) at the University of Memphis, the team used data from the ECOsystem Spaceborne Thermal Radiometer Experiment on Space Station (ECOSTRESS), Integrated Multi-Satellite Retrievals for Global Precipitation Measurement (GPM IMERG), and Landsat 8 Operational Land Imager (OLI) and Thermal Infrared Sensor (TIRS). The team also used ancillary data from the National Land Cover Database (NLCD) and the North American Land Data Assimilation System (NLDAS) Noah Land Surface Model. These results identified "thriving" recharge locations, which are areas most conducive to aquifer recharge in Fayette County. The partners may use the results to prioritize specific areas in need of protection before they become susceptible to the effects of urbanization and industrialization.

Key Terms

precipitation, evaporative stress, remote sensing, evaporative stress index, thriving index, land cover change, runoff

2. Introduction

2.1 Background Information

Groundwater depletion is a growing concern as the effects of increased agricultural activity, urbanization, and industrialization become apparent. In areas where groundwater is the primary water supply, it is vital to understand how this resource is replenished and what may endanger it. The Mississippi Embayment (ME) spans eight states in the southeast United States and is widely known for experiencing ground water depletion at a rapid rate (Ouyang et al., 2021). The Memphis Aquifer (MA), a part of the ME, supplies pristine water resources to Tennessee residents and for nearly all municipal, industrial, and agricultural needs in west Tennessee (TN Roadmap to Securing the Future of Our Water Resources, 2018). With an expected increase urbanization in Haywood and Fayette counties due to Ford's planned construction of their new battery assembly plant, Blue Oval City (BOC), replenishment of this water supply may be threatened due to the increased demand on the water supply and change in land cover type. An increase in impervious surfaces prevents precipitation from efficiently infiltrating and recharging the aquifer. While the runoff from impervious surfaces can eventually make its way into streams to recharge the aquifer—either naturally or from a drainage system—this water poses the threat of contaminating the aquifer with pollutants.

In examining water balance and evaporative stress in the area, the team can understand if excess water is running off and if the vegetation in the area is efficiently transpiring due to adequate water availability. In a related DEVELOP project—Mississippi Embayment Water Resources—it was determined that a thriving index pinpointing areas conducive to recharge would be a useful tool for the partners (Mahoney et al., 2022). By examining the aforementioned hydrological factors, the thriving index identifies locations where water can efficiently percolate down to the aquifer to recharge it, meaning there is adequate water available. Identifying these thriving areas in the aquifer recharge zone is important for conserving and protecting the MA so that these areas are prioritized for protection efforts before being affected by urbanization and industrialization. The study area focused on the Hatchie-Obion Watershed, paying close attention to BOC and its surrounding

counties, Haywood and Fayette (Figure 1). The area stretches across three states; Kentucky, Mississippi, and Tennessee, and covers approximately 25,000 km².

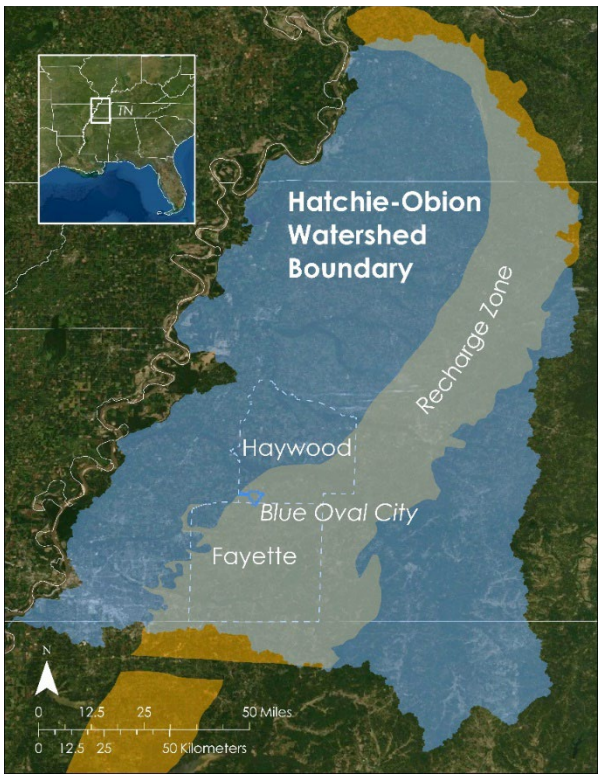

Figure 1. The study area of this project includes Ford's Blue Oval City, Haywood and Fayette Counties, the Hatchie-Obion Watershed (blue), and the Memphis Aquifer's Recharge Zone (orange)

2.2 Scientific Basis

In order to identify water stressed areas, it is vital to consider the factors that directly affect recharge in the MA which include precipitation (P), evapotranspiration (ET), the evaporative stress index (ESI), land cover type, and runoff—all of which influence recharge rate and can impact water stressed areas (Mohan et al., 2018). Precipitation—followed by evapotranspiration—is the largest global contributor to the water cycle (Cawse-Nicholson et al., 2020). P influences the presence of surface water, which can directly percolate down through the vadose zone to recharge the aquifer—especially in rural regions. In seasons with low P, agricultural areas increase their reliance on groundwater to maintain crop irrigation. ET, a combination of evaporation and plant transpiration, is an indicator of vegetation stress. When plants do not have access to water, their stomata close and reduce their transpiration rate, which increases their temperature. The ECOSTRESS instrument, located on the International Space Station, detects this increase in plants' temperature when water stressed (Cawse-Nicholson et al., 2020). As a result, ET also influences how much P is available to become surface water. The construction of BOC will alter the land cover type and may impact the recharge rate due to the expansion of impervious surfaces (Smith, 2019). ESI is an indicator of potential plant water stress by highlighting areas where plant productivity is poor. Accurate estimation of these factors can provide insights into spatiotemporal changes in water availability.

2.3 Previous Term

In the spring 2022 term Mississippi Embayment Water Resources project, the team utilized various Earth observations, including the Terra Moderate Resolution Imaging Spectrometer (MODIS), Gravity Recovery and Climate Experiment (GRACE), and GPM IMERG to find thriving areas within the entire ME. A positive value for water balance is an indicator of a thriving area because it implies that the excess water may

run off to streams and has the potential to recharge the aquifer. An ESI value closer to 1 is another indicator of a thriving area because it shows how vegetation is efficiently transpiring. The thriving areas were located by comparing water balance and ESI maps along with land cover data. The previous team constructed a methodology framework to allow the current team to zoom in on the west Tennessee portion of the aquifer by incorporating higher resolution data from ECOSTRESS for a more detailed view of the thriving areas within the west Tennessee portion of the aquifer.

2.4 Project Partners & Objectives

Protect Our Aquifer (POA) is a nonprofit advocacy group interested in using Earth observations (EO) to aid their groundwater monitoring efforts and to help educate policymakers and Tennesseans about the importance of conserving the MA. POA relies on ground-based monitoring and uses some GIS mapping techniques but does not currently utilize any EO in their work. POA is particularly interested in how they can implement EO data in their long-term monitoring efforts, particularly due to the expected consequences of new development in the area—such as the construction of BOC. The creation of a thriving index from the P, land cover, ET, and ESI will allow POA to identify areas in the west Tennessee portion of the aquifer in need of protection.

In an expanded partnership with POA and The Center for Applied Earth Science and Engineering Research (CAESER) at the University of Memphis, this project assessed water availability and vulnerability in the west Tennessee portion of the MA by investigating P data acquired from GPM IMERG, ET and ESI from ECOSTRESS, and land cover datasets from the NLCD and Landsat 8 OLI and TIRS. These data, along with ancillary data sets, would ultimately be used to create a water balance map and thriving area index (Table 1 and Table 2). The thriving area index allowed for identification of areas in need of conservation and protection to their thriving characteristics, such as favorable water balance and land cover values.

Table 1. *List of sensors and data products utilized for this project*

Platform and Sensor	**Data Product**	**Parameters**	**Dates**	**Acquisition Method**
ISS ECOSTRESS	ECOSTRESS Evapotranspiration dis-ALEXI Daily L3 CONUS 70 m V001 ECOSTRESS Evaporative Stress Index dis-ALEXI Daily L4 CONUS 70 m V001	Evapotranspiration, Evaporative stress index	March 2019-August 2022	LP DAAC AppEEARS
GPM IMERG	GPM IMERG Final Precipitation L3 1 month 0.1 degree x 0.1 degree V06 GPM IMERG Late Precipitation L3 1 day 0.1 degree x 0.1 degree V06	Monthly averaged precipitation Daily accumulated precipitation	March 2019-August 2021 September 2021 – August 2022	EarthData - Giovanni
Landsat 8 OLI and TIRS	USGS Landsat 8 Level 2, Collection 2, Tier 1	Land cover	January 2019-August 2022	Google Earth Engine Data Catalog

Table 2. *Ancillary datasets used for land classification maps, runoff analysis, and reference maps*

Agency	**Data Product**	**Purpose**	**Acquisition Dates**	**Acquisition Method**
US Census TigerLine	US state county lines	Contextual boundary for study area	September 2022	US Census Bureau
USGS - National Hydrography Dataset	USGS National Hydrography Dataset Plus High Resolution (NHDPlus HR) for 4-digit Hydrologic Unit - 0801	Watershed boundary for the study area	October 2022	USGS The National Map download client.
National Land Cover Database (NLCD)	Land cover dataset	Used to identify land cover and impervious land cover types to create a thriving index	October 2022	NLCD
North American Land Data Assimilation System	Noah Land Surface Model	Used to examine surface and subsurface runoff seasonally	October 2022	EarthData

3. Methodology

3.1 Data Acquisition

To obtain the shapefiles of the study area—Haywood and Fayette counties—the national county US Census Bureau dataset was downloaded from TigerLine. The team selected the two counties and merged them into one shapefile. Since political boundaries may not fully represent the ecological phenomenon in question—groundwater recharge—the team extended the study area to align with the watershed Hydrological Unit Code 6 (HUC-6) boundary obtained from United States Geological Survey's (USGS) "The National Map" download client.

The Final Run of GPM IMERG v06 precipitation data (FRM)—which captures monthly precipitation data—was downloaded from NASA's EarthData Giovanni portal. The team selected the "Time Average Map" plot. The date ranges input matched the first day of the seasonal range to the last day of the season's range in order to maintain consistency for the time frame. The ranges selected for the seasons were: Winter: December 1 to February 28; Spring: March 1 to May 31; Summer: June 1 to August 31; Fall: September 1 to November 30.

In September 2019, GPM IMERG temporarily discontinued the monthly precipitation dataset with a new release date in early 2023. To solve this gap in data acquisition—from September 2019 to August 2022—the team used the Late Run of GPM IMERG v06 precipitation daily data (LRD) which was also downloaded

from NASA's EarthData Giovanni portal with the same steps as the FRM data. LRD is computed approximately 14 hours after its observation time, whereas the FRM is processed approximately 3.5 months after the observation time and includes monthly gauge analyses (GES DISC, n.d.). To understand how P may contribute to excess water, the team examined runoff data from the monthly North American Land Data Assimilation System (NLDAS) Noah lLand Surface Model by downloading from EarthData.

ECOSTRESS level 3 evapotranspiration and level 4 ESI products along with their associated quality flags were downloaded from The Land Processes Distributed Active Archive Center Application for Extracting and Exploring Analysis Ready Samples (LP DAAC AppEEARS) as GeoTIFF files. For additional monitoring of uncertainties in the data, ECOSTRESS level 2 surface temperature and emissivity quality control layers were downloaded as GeoTIFF files. Data were clipped to the study area before downloading.

Surface reflectance and land surface temperature data from the Landsat 8 OLI and TIRS sensors were imported from the Google Earth Engine (GEE) data catalog. To monitor changes in landcover the team imported the USGS NLCD from the GEE catalog. While Landsat 9 data are available for some of the study period, the team did not incorporate this data because Landsat 8 has coverage for the entire study period.

3.2 Data Processing

3.2.1 Evapotranspiration and Evaporative Stress Index

The team processed ET and ESI data in Python 3.9.12. Fill values for missing data—in addition to values greater than 1000 mm/day and less than 0 mm/day in the ET raster—were replaced with NaN (not a number; pixels with no data) from the analysis, as the expected ET rate is between 0 and 10 mm/day. Keeping these pixel values would skew the results. ET raster pixels were also replaced with NaN when the pixel values of the quality flag and quality control layers were not equal to 0 mm/day. Pixel values below the 8th quantile and above the 98th quantile were categorized as outliers and also removed from the analysis. After an initial round of processing, specific processed images contained large areas with a pixel value of 0.1 mm/day, which indicated undetected cloud cover. As a result, the team created an additional processing step to replace pixel values equal to 0.1 to NaN. The team removed images with more than 80% missing pixels and computed the seasonal averages with rasters containing fewer than 80% missing pixels.

When using a large study area, data are not always collected for the entire area as frequently as it would be for a smaller area because of the size of the swath. As a result, the team utilized partially complete images to ensure the maximum possible data preservation to create the seasonal composites. For that reason, the team set the threshold of the missing pixels to 80%. The composites were then created by merging all the data arrays and then calculating the mean of those arrays. To visualize the processed imagery, the team exported the raw imagery as GeoTIFF files and imported them into ArcGIS Pro 2.9.3. The ESI products followed a similar workflow. For ESI, if the processed image was composed of only pixel values equal to 0, those images were manually removed from the analysis. The water balance equation included the final processed evapotranspiration images.

3.2.2 Precipitation

The team used FRM and LRD to create averaged seasonal maps utilizing the NASA Goddard Earth Sciences Data and Information Services Center (GES DISC) Giovanni web app. To create the seasonal average from FRM for 2019 to 2021, we selected each month for each season, plotted them in Giovanni (e.g., March, April, and May for Spring), and continued with each year. The team drew a bounding box encompassing the study area, and the units for GPM IMERG were changed to mm/day to match the units of ECOSTRESS data. After plotting the data, the team downloaded the precipitation data in a GeoTIFF format for further processing in ArcGIS Pro. GES DISC paused the post-processing of FRM for dates after September 2019. To complete the data gap for the remaining seasons, the team used LRD and the same method in Giovanni to plot the averaged seasonal maps.

The spatial resolution for GPM IMERG is very coarse at 10km x 10km, whereas ECOSTRESS is more detailed at 70m x 70m. To match the spatial resolutions, the team first clipped the GPM IMERG images to the study area extent. The team then rescaled GPM IMERG to match ECOSTRESS using ArcGIS Pro's rescale raster function. Afterward, both datasets from GPM IMERG and ECOSTRESS were ready for analysis.

3.2.3 Water Balance

The team used the Model Builder tool in ArcGIS Pro to iterate each raster and clip them to the HUC study area. To calculate the water balance, the team utilized Equation 1, where P refers to the GPM IMERG precipitation imagery, and ET refers to the evapotranspiration imagery acquired from ECOSTRESS. Equation 1 is a simplified version of water balance that analyzes water stress vulnerability (Cui et al., 2022). To create the new water balance raster images for each season, the team calculated the processed precipitation images from GPM IMERG and the evapotranspiration images from ECOSTRESS using the "Raster Calculator" geoprocessing tool in ArcGIS Pro 2.9.3. The output water balance images were then adjusted to a uniform scale of -3 mm/day as the minimum value and 8 mm/day as the maximum value.

$$Water\ balance = P - ET \quad (1)$$

3.2.3 Land Cover

The team adopted the land cover workflow from a previous DEVELOP project, Huntsville Urban Development (Paris, et al. 2020). First, the team processed Landsat 8 data in GEE by cloud masking to filter out any unusable images. For each year of Landsat 8 imagery, the median of each band was selected. NLCD data were then remapped to group the NLCD classifications into four broader groups: water, pervious surfaces, trees, and developed. Pervious surfaces included grasslands, shrublands, sedge and herbaceous land, lichens, moss, and pastures. See table G1 for exact band selection for each remapped class. Next, the team sampled the remapped 2019 NLCD data and 2019 Landsat 8 imagery together to get a feature collection of training data. In this step, the team also filtered out any null or no data pixels. The team then performed an unsupervised classification by making a random forest classifier with the feature collection data. This random forest classifier was used to classify each year of Landsat 8 imagery to the remapped NLCD bands. To test the accuracy of the training data, the team ran a confusion matrix with the random forest classifier. To get validation data, the 2019 Landsat 8 imagery and NLCD were sampled again with a random seed generator. These validation data were then classified and run through a confusion matrix to get the expected accuracy. Data were clipped to the Hatchie-Obion watershed and the rasters of each year of reclassified Landsat 8 data were exported out of GEE for visualization in ArcGIS Pro.

3.2.4 Runoff

To examine runoff at a seasonal scale, the team downloaded monthly runoff data from the Noah Land Surface Model from the NLDAS. For each month, the team added together the monthly surface runoff (Qs layer) and subsurface runoff (Qsb layer) raster layers to generate one raster to represent total runoff for each month in ArcGIS Pro. To get a seasonal value, the team averaged together the runoff for each of the months in each season. For example, for spring seasons the runoff rasters for March, April and May were added together and then divided by three to get the average spring runoff.

4. Results

4.1 Data Analysis

4.1.1 Evaporative Stress Index

The team plotted seasonal ESI in ArcGIS Pro to assess overall spatiotemporal trends across the study area, paying particular attention to Fayette & Haywood counties. The plots assisted in identifying areas where vegetation is experiencing water stress. The team also plotted average seasonal ESI across the four-year period in Python Plotly to assess changes in average ESI over time (Figure 2).

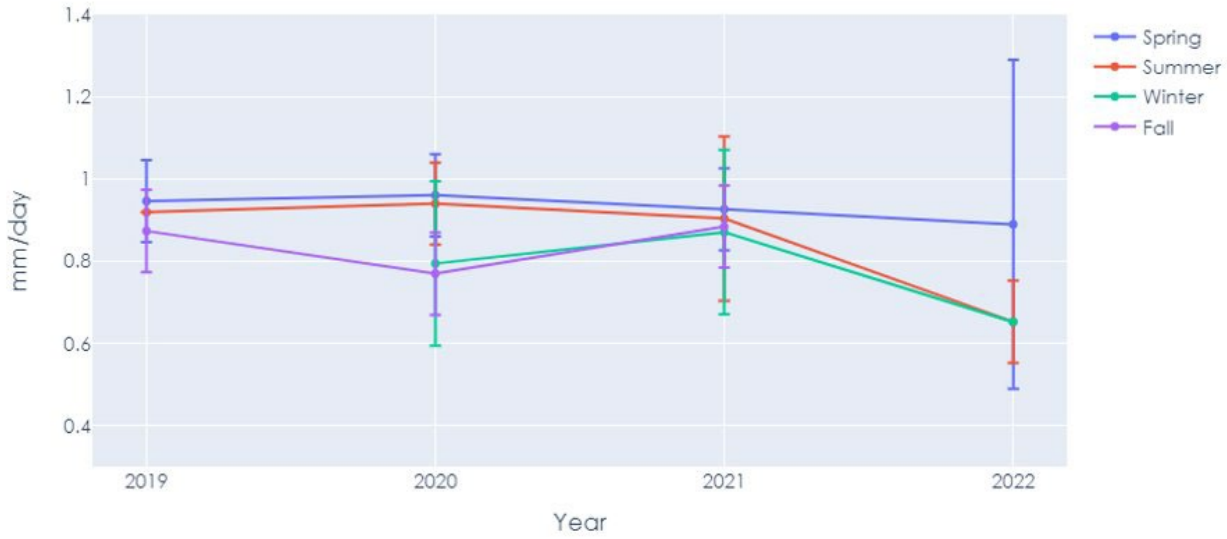

Figure 2. Average seasonal Evaporative Stress Index values from 2019 through 2022

4.1.2 Water Balance

The team plotted a time series of the seasonal changes in water balance from Spring 2019 to Summer 2022 to assess trends and visualize changes over the study period (Figure 3). Figure 3 displays a water balance time series, showcasing the range between the lowest and highest water balance value for each season. The season with the greatest range in water balance was Summer 2021 and the lowest range of water balance values was from Winter 2020. The Summer seasons range from around -4 to 5 mm/day. Fall also showed a consistent trend. Spring water balance range fluctuates the most.

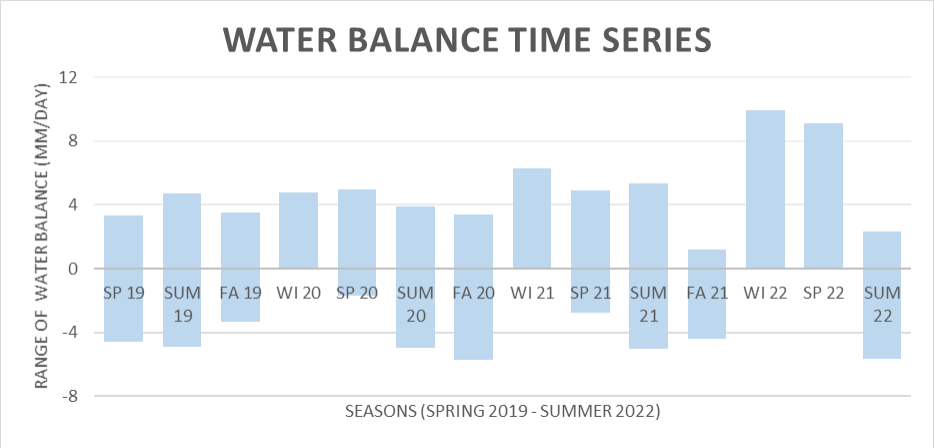

Figure 3. Water balance time series from Spring 2019 to Summer 2022

4.1.3 Land Cover

The team conducted a statistical analysis to understand which land cover types had a percent increase or decrease. To start, the number of pixels of each land cover type in each NLCD raster were calculated to their respective coverage in square kilometers. From there, a percent change calculation was performed with the 2019 and 2022 land cover type values. The amount of coverage of each land cover type in square kilometers from 2019 and 2022 across the entire study area with the percent change between the two years. There is a greater decrease in pervious surfaces than impervious surfaces (Table 3). Decreases in land cover types and lack of land pixels from 2022 data may result from the team only accessing partial data for 2022, up to August, while the team had a full year's worth of data for the year 2019.

Table 3. *Land cover change over the study area*

	2019 (Land Cover in sq km)	2022 (Land Cover in sq km)	Percent Change
Trees	87173.73	58915.34	32.42% decrease
Pervious	50712.04	40328.94	20.47% decrease
Impervious	685.47	656.98	4.16% decrease
Water	38.42	41.73	8.62% increase

4.1.4 Runoff

The team mapped each season of runoff data in ArcGIS Pro to visualize where excess runoff was occurring in the study area. The team also plotted each season of runoff for each year to graphically assess trends in runoff. The maps and graphs were also used when comparing land cover, ET, and ESI maps to make connections between these variables and excess runoff.

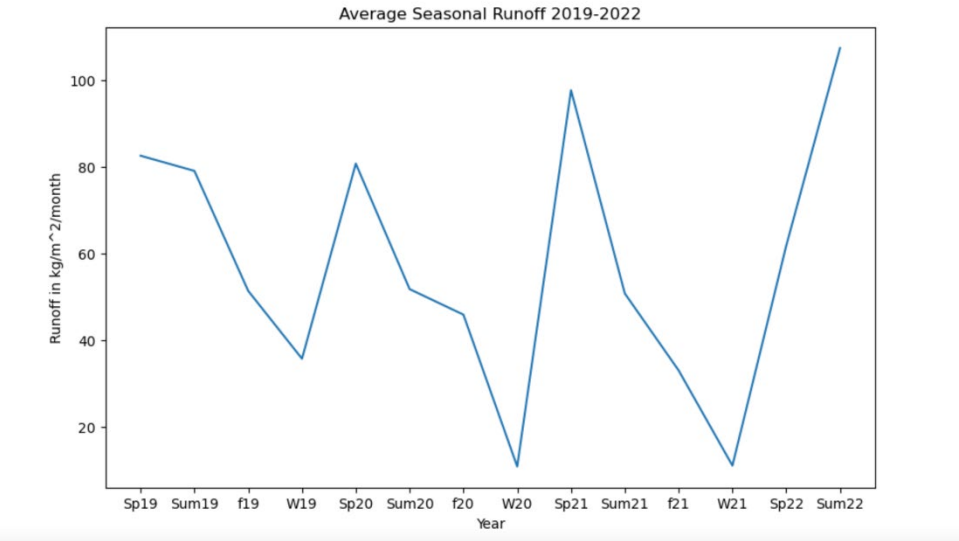

Figure 4. Average seasonal runoff from 2019 to 2022

4.1.5 Thriving Areas

The team compared water balance, ESI, land cover, and runoff maps to pinpoint areas in need of conservation. Using this map, the team identified locations with abundant and healthy vegetation where water can efficiently percolate down to the aquifer to recharge it. The land cover map shows Fayette County in the region of the recharge zone with a land cover of mainly pervious surface. The darker blue colors from ESI illustrates high levels of ESI. In addition, there is run off in these areas and the water balance has yellow and green areas which indicate positive water balance values.

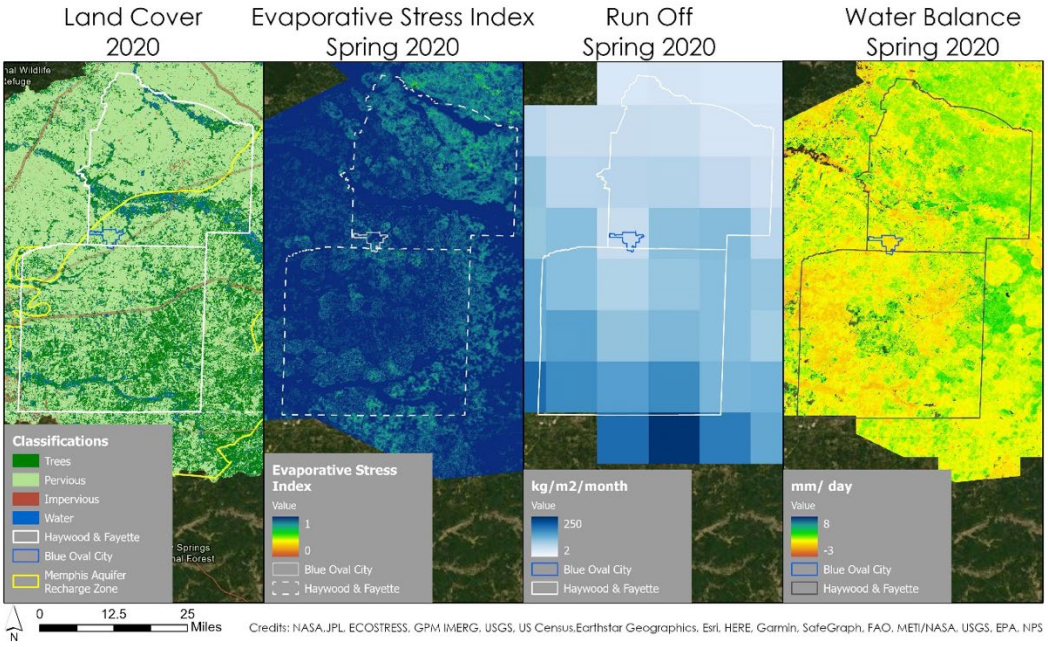

Figure 5. A map of the components that can be used to determine whether an area is thriving.

4.2 Analysis of Results

4.2.1 ET and ESI

The seasonal raster plots of ECOSTRESS ET were composed of approximately six raster images on average with the highest for Summer 2019, with 17 images and the lowest for Spring 2022 with one image. The seasonal composites for ECOSTRESS ESI were composed of approximately eight images on average with the highest for Summer 2019 with 16 images and the lowest for Winter 2020 with one image. Weather was a significant determining factor for the number of images available; during periods of higher cloud cover there were fewer images. As a result, there is some uncertainty in the accuracy of the results presented in the images. In Figure 6, the error bars help with visualizing which seasons may be more accurate. The error bars were calculated by multiplying the ratio of the number of images expected to the number of images observed and the highest number of valid pixels to the number of valid pixels observed, followed by applying a scale factor (1/10). The expected number of images was determined by taking an average of the images observed per season. The expected pixel quantity was determined by the season with the highest number of valid data. Figure 6 displays average evapotranspiration across all seasons and years. The highest ET average was observed in Spring 2019, closely followed by Summer 2019, while the lowest ET average was observed in Summer and Winter 2022. Apart from the Fall seasonal averages, overall ET decreased throughout the four-year period.

Figures E1, E2, F1, and F2 depict the average ET across the entire study area. ET is typically highest in the spring and summer seasons and decreases by the end of fall and winter. These trends can be observed in Figure 6 where higher averages of ET were observed during the spring and summer months. ET depends on several factors, such as temperature, cloud cover, water availability, and vegetation type, so the patterns are not always uniform season to season and year to year. As expected, ET values varied across season and year. The spring plots in Figure A1 demonstrate a significant drop in ET across the entire study area, but particularly in the east and south-east. In the summer and fall seasons, ET was similarly lower in the southern region (Figure E2 and Figure F2).

Spring had the highest average ESI (Figure 2). Summer had a similarly high average ESI between 2019 and 2021 but decreased by 2022. These results align with the ET findings, higher productivity in summer and

spring. Figures C1, C2, D1, and D2 depict the average ESI across the entire study area. The ESI was distinctly lower in the northern part of the study area across all seasons. Similarly, to the ET results, certain seasons also exhibited displayed lower productivity in the south-east.

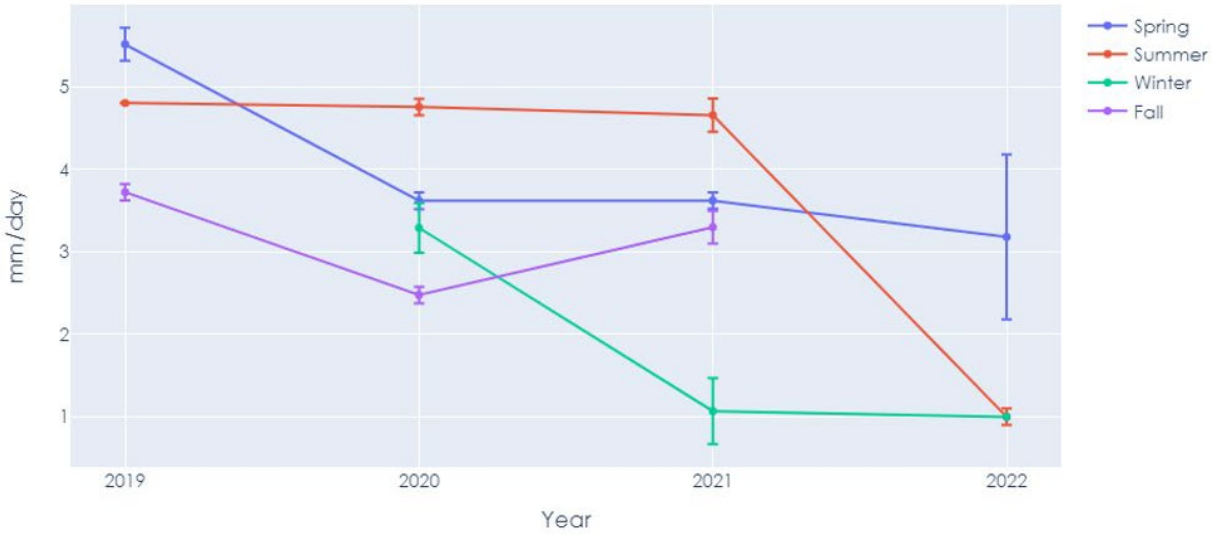

Figure 6. Seasonal average evapotranspiration from 2019 through 2022.

4.2.2 Water Balance

The results in Figure 3 show that each Summer tends to have a range of water balance values that start in the negative range. This is indicative of the decrease in precipitation and the increase of ET. The Winter water balance values are generally more positive, which can be directed to the lower ET and higher precipitation in these months. Figures A1, A2, B1, and B2 depict the water balance across the entire study area. Overall, the water balance plots demonstrated that the inflows and outflows of water were similar. Spring 2020 and 2021 were the only seasons where precipitation values were higher than ET. In most of the other seasons, the water balance was slightly above 0 mm/day and negative mm/day.

5. Discussion and Conclusions

5.1 Results Discussions

5.1.1 Evaporative Stress Index

ESI was relatively high across all four years. Areas with high ESI, closer to 1, depict vegetation that is transpiring close to its potential. In such areas, plants are receiving a sufficient amount of water and efficiently transpiring. For that reason, high ESI is an indicator of thriving region. On the other hand, values closer to zero indicate that vegetation is not receiving sufficient water resources and they are becoming water stressed.

5.1.2 Water Balance

Low water balance indicates areas where P and ET are approximately equal. When they are equal, little water is left to recharge the aquifer. Thus, a healthy water balance is when ET is slightly lower than P. A high water balance is concerning as it indicates less plant uptake of water. Higher water balance values are expected to be present in urban areas with impervious surfaces, as rainfall turns to runoff and is not able to percolate into the ground. A negative water balance value is when there is an excess amount of evapotranspiration, which suggests that vegetation is getting its water from either runoff or irrigation. A negative water balance is concerning as it could mean groundwater resources are being depleted as it is used to irrigate the area.

5.1.3 Thriving Areas

Based on the seasonal water balance analysis, evaporative stress maps, land cover change, and runoff models, the team identified Fayette County as a thriving area for further conservation. Fayette County is located within the recharge zone and the land cover in this area is predominantly pervious. These geographical features allow surface water to directly percolate into the aquifer. Furthermore, areas where the water balance is between 1-2 mm/day suggests that plants efficiently use up available water resources while having some water left to potentially recharge the aquifer. The water balance for this area was found to be in that range. There is also a network of streams within the identified thriving area where precipitation and runoff can laterally recharge the aquifer. In addition, the southern portion of the county has higher levels of runoff, which can supply the stream, and the remainder can percolate into the aquifer. The ESI was also high, meaning that vegetation is receiving a sufficient amount of water and efficiently transpiring. In addition to meeting these criteria, BOC is within these counties making it an area of concern for further monitoring. When comparing all of the factors across the entire study area, Fayette County appeared to be the most conducive to recharge.

5.2 Future Work

The LRD data was a workaround for the missing FRM data for the seasons from September 2021 and August 2022. For future work, the team recommends utilizing this methodology to apply the FRM data from 2022 when it becomes available from GES DISC in early 2023. The preliminary results that were generated from LRD during the 2021 to 2022 seasonal analysis can then be compared to seasonal analysis using the newly acquired FRM data. The data from ECOSTRESS was also limited for the winter and the seasons in 2022, as most of the images were affected by clouds. Considering the climate of the study area, Synthetic Aperture Radar (SAR) might be something to consider for future projects since it can penetrate through the clouds. SAR data would also be beneficial to understand ground subsidence in the region, which would help future teams understand if the water table has significantly changed over time. The water balance equation was simplified to ensure the feasibility of completing the project on time; for a future project, it would be beneficial to explore other factors that influence groundwater recharge. The ESI results could be used to identify areas that may require additional inputs of water in the future as a result of drought. These inputs may increase reliance on the aquifer for water resources. The team recommends adding NASA's Gravity Recovery and Climate Experiment (GRACE) Earth observation sensor to this project and consider creating a suitability map by combining all the datasets into one map that will accurately reveal areas with high and low water storage.

5.3 Conclusion

This project demonstrated the use of NASA Earth observations to assess water availability and vulnerability in the MA. The team determined that areas where the water balance is low, ESI is high, runoff is high, and there is mainly pervious land cover, recharge can effectively take place. Identification of effective recharge locations may be used by the partners to prioritize areas in need of protection before they become victim to industrialization and urbanization.

6. Acknowledgments

The team would like to thank everyone for their support and guidance in the Western Tennessee Water Resource project. This research was made possible by funding from Space System and Applications, Inc. The team would especially like to thank science advisors Kerry Cawse-Nicholson, Madeleine Pascolini-Campbell, and Benjamin Holt at NASA Jet Propulsion Laboratory, California Institute of Technology, and Kathleen Lange, their NASA DEVELOP JPL Fellow.

A special thanks to the team's project partners who provided resources and expertise throughout this project. The team would also like to thank Sarah Houston (Executive Director), Ward Archer (President), and Jim Kovarik (Board Member) from Protect Our Aquifer. Additionally, the team appreciated the collaboration and guidance from Brian Waldron (Director), and Scott Schoenfernacker (Associate Director) from The Center for Applied Earth Science and Engineering Research at the University of Memphis. The team would also like to thank the Tennessee department of Environment and conservation, specifically Brian Ham, for their technical guidance and expertise.

Any opinions, findings, and conclusions or recommendations expressed in this material are those of the author(s) and do not necessarily reflect the views of the National Aeronautics and Space Administration.

This material is based upon work supported by NASA through contract NNL16AA05C.

7. Glossary

Earth observations – Satellites and sensors that collect information about the Earth's physical, chemical, and biological systems over space and time
ECOSTRESS – ECOsystem Spaceborne Thermal Radiometer Experiment
GPM IMERG – Global Precipitation Measurements - Integrated Multi-Satellite Retrievals for GPM
Evapotranspiration (ET) – The sum of evaporation from the land surface plus transpiration from plants
Evaporative Stress Index (ESI) - Highlights areas with unusually high or low rates of water use across the land surface.
Water balance – The result of the equation subtracting evapotranspiration from precipitation (P – ET); a measure comparing inflows (precipitation) and outflows (ET) in the water system
Vadose zone – Unsaturated zone spanning from the ground surface to the water table.
Thriving area - Locations where water can efficiently percolate down to the aquifer to recharge it, meaning areas with healthy and abundant vegetation and pervious ground.
FRM – Final Run Monthly GPM IMERG precipitation data; data taken 3.5 months after observations period
LRD – Later Run Daily GPM IMERG precipitation data; data taken 14 hours after observation period
GES DISC – NASA's Goddard Earth Science Data and Information Services Center
LP-DAAC – NASA's Land Processes Distributed Active Archive Center
GIOVANNI – GES DISC's web application that provides a convenient way to access, visualize, and analyze remote sensing data.
Time series – A graph displaying change in values over time.

9. References

Byrne, M., O'Gorman, P.A. (2015) The Response of Precipitation Minus Evapotranspiration to Climate Warming: Why the "Wet-Get-Wetter, Dry-Get-Drier" Scaling Does Not Hold over Land. *Journal of Climate,* 8078-8092. https://doi.org/10.1175/JCLI-D-15-0369.1

Cawse-Nicholson, K., Braverman, A., Kang, E. L., Li, M., Johnson, M., Halverson, G., Anderson, M., Hain, C., Gunson, M., & Hook, S. (2020). Sensitivity and uncertainty quantification for the ECOSTRESS evapotranspiration algorithm – DisALEXI. *International Journal of Applied Earth Observation and Geoinformation*, *89*, 102088. https://doi.org/10.1016/j.jag.2020.102088

CAESER - University of Memphis. (2021, October 6). *The Memphis Aquifer.* https://caeser.memphis.edu/resources/memphis-aquifer/

Cui, G., Ma, Q., Bales, R. (2022). Assessing multi-year-drought vulnerability in dense Mediterranean-climate forests using water-balance-based indicators. *Journal of Hydrology*, Volume 606, 127431, ISSN 0022-1694, https://doi.org/10.1016/j.jhydrol.2022.127431.

Hook, S., Hulley, G. (2019). *ECOSTRESS Land Surface Temperature and Emissivity Daily L2 Global 70 m V001.* NASA EOSDIS Land Processes DAAC. Accessed 2022-10-11 from https://doi.org/10.5067/ECOSTRESS/ECO2LSTE.001 Accessed October 11, 2022.

Hook, S., Cawse-Nicholson, K. (2021). *ECOSTRESS Evaporative Stress Index dis-ALEXI Daily L4 CONUS 70 m V001.* NASA EOSDIS Land Processes DAAC. Accessed 2022-10-02 from https://doi.org/10.5067/ECOSTRESS/ECO4ESIALEXI.001. Accessed October 2, 2022.

Hook, S., Cawse-Nicholson, K. (2021). *ECOSTRESS Evapotranspiration dis-ALEXI Daily L3 CONUS 70 m V001.* NASA EOSDIS Land Processes DAAC. Accessed 2022-10-11 from https://doi.org/10.5067/ECOSTRESS/ECO3ETALEXI.001. Accessed October 11, 2022.

Huffman, G.J., E.F. Stocker, D.T. Bolvin, E.J. Nelkin, Jackson Tan (2019), *GPM IMERG Final Precipitation L3 1 month 0.1 degree x 0.1 degree V06*, Greenbelt, MD, Goddard Earth Sciences Data and Information Services Center (GES DISC), Accessed: Oct 2022, 10.5067/GPM/IMERG/3B-MONTH/06

Huffman, G.J., E.F. Stocker, D.T. Bolvin, E.J. Nelkin, Jackson Tan (2019), *GPM IMERG Late Precipitation L3 1 day 0.1 degree x 0.1 degree V06*, Edited by Andrey Savtchenko, Greenbelt, MD, Goddard Earth Sciences Data and Information Services Center (GES DISC), Accessed: Oct 2022, 10.5067/GPM/IMERGDL/DAY/06

Mahoney, L., Hatch, B., Villanueva-Weeks, C., & Webster, L. (2022). *Mississippi Embayment Water Resources: Utilizing NASA Earth Observations to Understand Groundwater Recharge in the Mississippi Regional Aquifer System.* NASA DEVELOP National Program, California – JPL. https://ntrs.nasa.gov/api/citations/20220005934/downloads/2022Spring_JPL_MississippiEmbaymentWater_TechPaper_FD_v4.docx

Ouyang, Y., Wan, Y., Jin, W., Leininger, T., Feng, G., & Han, Y. (2021). *Impact of Climate Change on*

Groundwater Resource in a Region with a Fast Depletion Rate: the Mississippi Embayment. Journal of Water and Climate Change, 6(12). https://doi.org/10.2166/wcc.2021.326

Paris, G., Nix, S., Quintero, T., & Tomlinson, A. (2020). *Huntsville Urban Development: Utilizing NASA Earth Observations to Evaluate Urban Tree Canopy and Land Surface Temperature for Green Infrastructure Development and Urban Heat Mitigation in Huntsville, AL.* NASA DEVELOP National Program, Alabama – Marshall. https://ntrs.nasa.gov/api/citations/20205008333/downloads/2020Sum_MSFC_HuntsvilleUrban_TechPaper_FD-final.docx.pdf

TNH$_2$O. (2018). *Tennessee's Roadmap to Securing the Future of Our Water Resources.* https://cumberlandrivercompact.org/wp-content/uploads/2019/10/TN_H2O_REPORT.pdf

TN Office of the Governor. (2021, September 27). *Memphis Regional Megasite Lands $5.6 Billion Investment from Ford Motor Company and SK Innovation* https://www.tn.gov/governor/news/2021/9/27/memphis-regional-megasite-lands--5-6-billion-investment-from-ford-motor-company-and-sk-innovation.html

US Census Bureau. (n.d.). *2021 Tiger/Line® shapefiles: Counties+(and+equivalent).* United States Census Bureau. Retrieved October 14, 2022, from https://www.census.gov/cgi-bin/geo/shapefiles/index.php?year=2021&layergroup=Counties%2B%28and%2Bequivalent%29

U.S. Census Bureau *Quickfacts: Haywood County, Tennessee.* United States Census Bureau. (n.d.). https://www.census.gov/quickfacts/fact/table/haywoodcountytennessee/PST045221

U.S. Geological Survey, National Geospatial Program, 20221010, *USGS National Hydrography Dataset Best Resolution (NHD) for Hydrological Unit (HU) 4 - 0801* (published 20221010) Shapefile: U.S. Geological Survey.

U.S. Geological Survey (2020). *Landsat 8-9 OLI/TIRS Collection 2 Level-2 Science Products.* USGS Earth Resources Observation and Science (EROS) Center. Accessed October 2022. https://doi.org/10.5066/P9OGBGM6

Appendix A

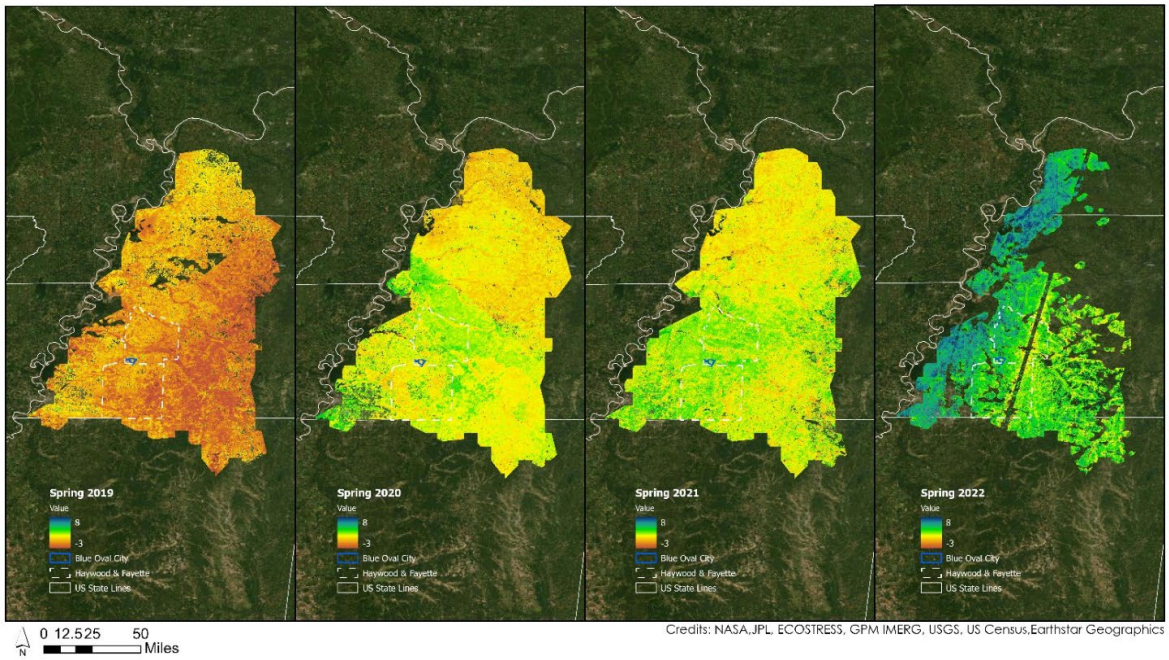

Figure A1 Spring Seasonal Water Balance

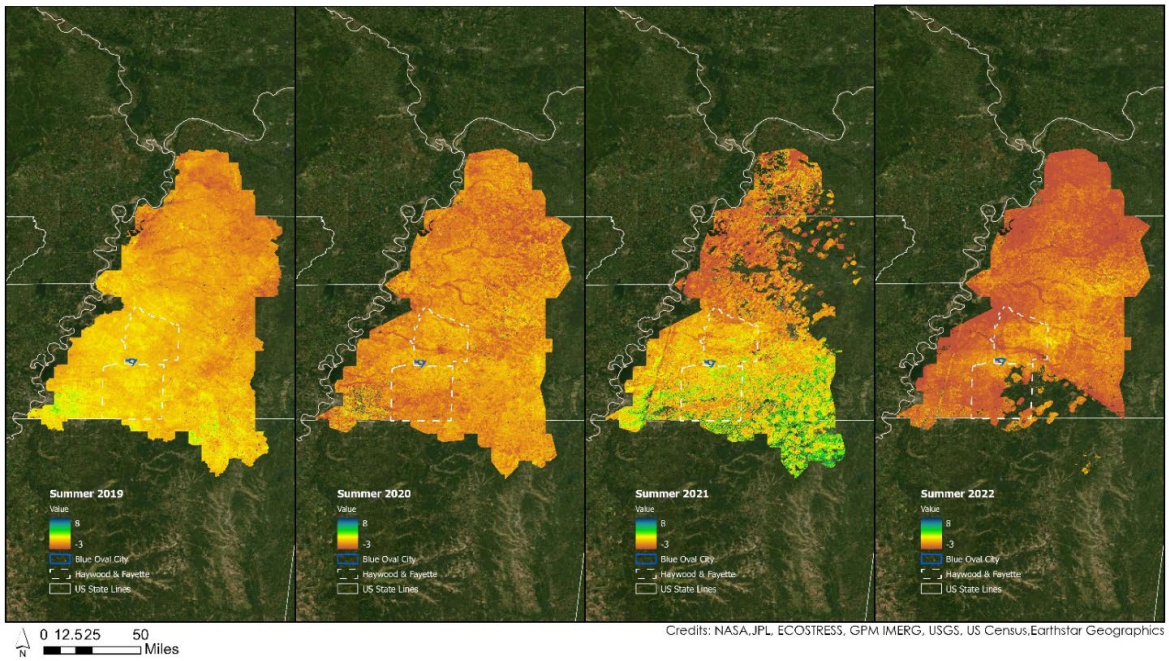

Figure A2 Summer Water Balance

Appendix B

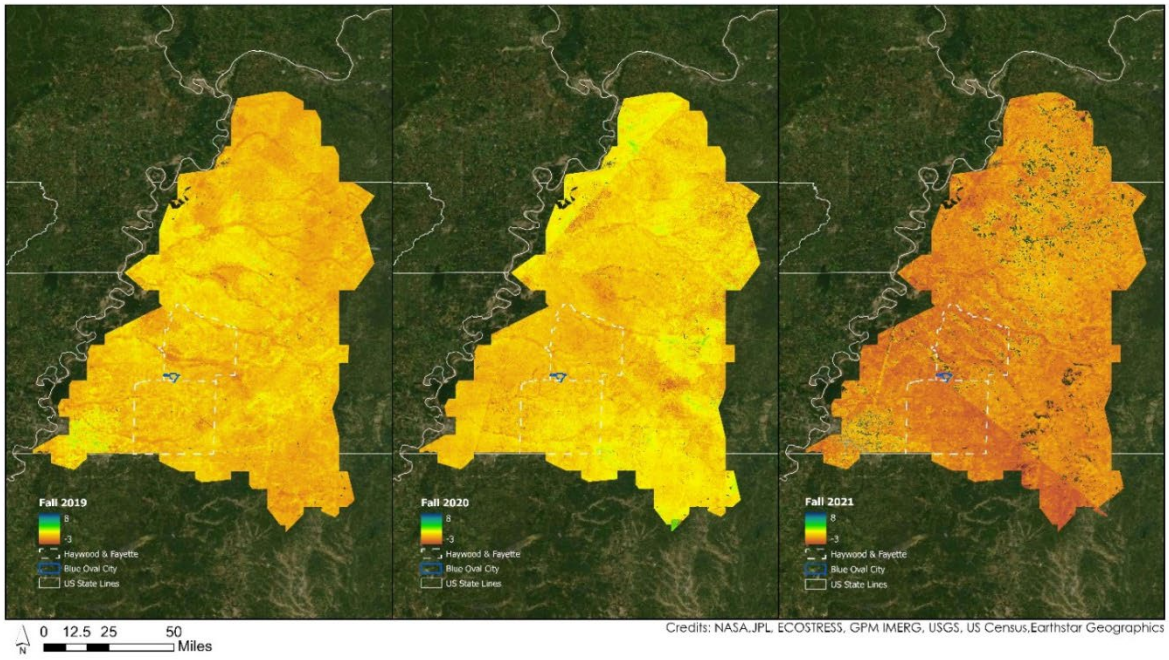

Figure B1 Fall Seasonal Water Balance

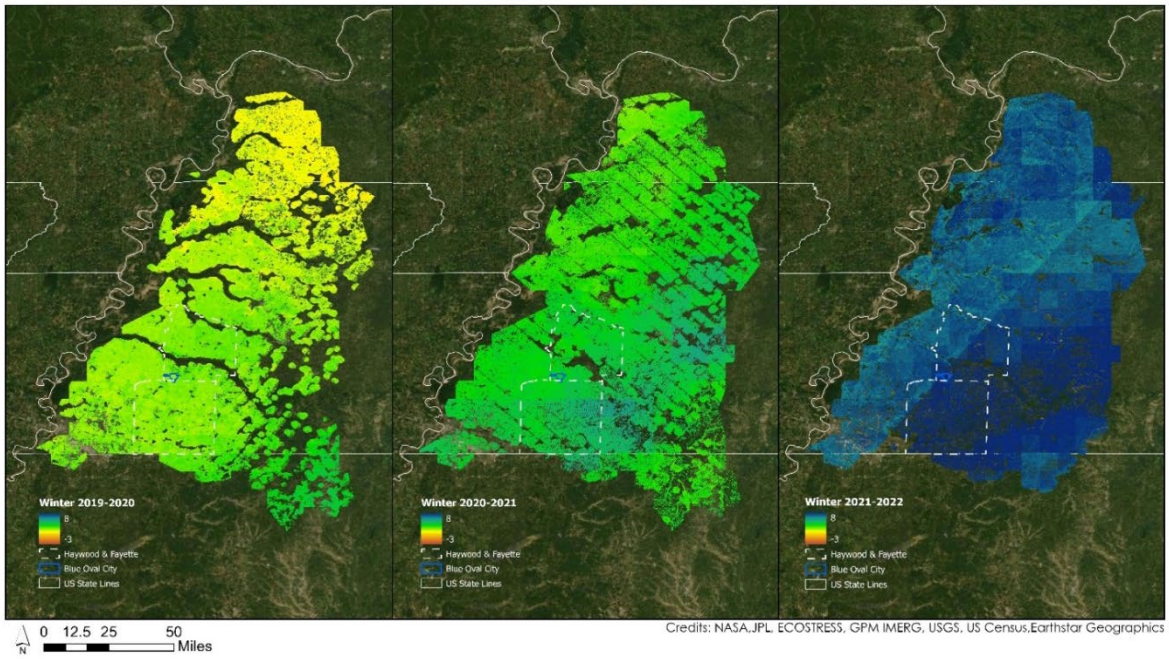

Figure B2 Winter Seasonal Water Balance

Appendix C

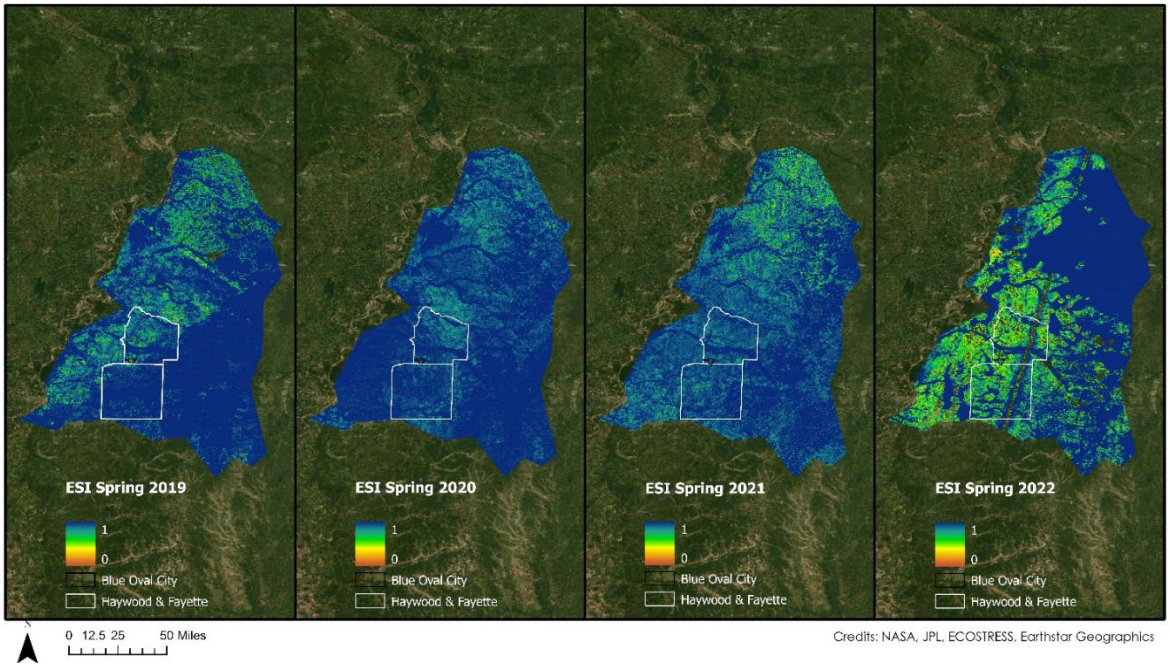

Figure C1 Spring Evaporative Stress Index

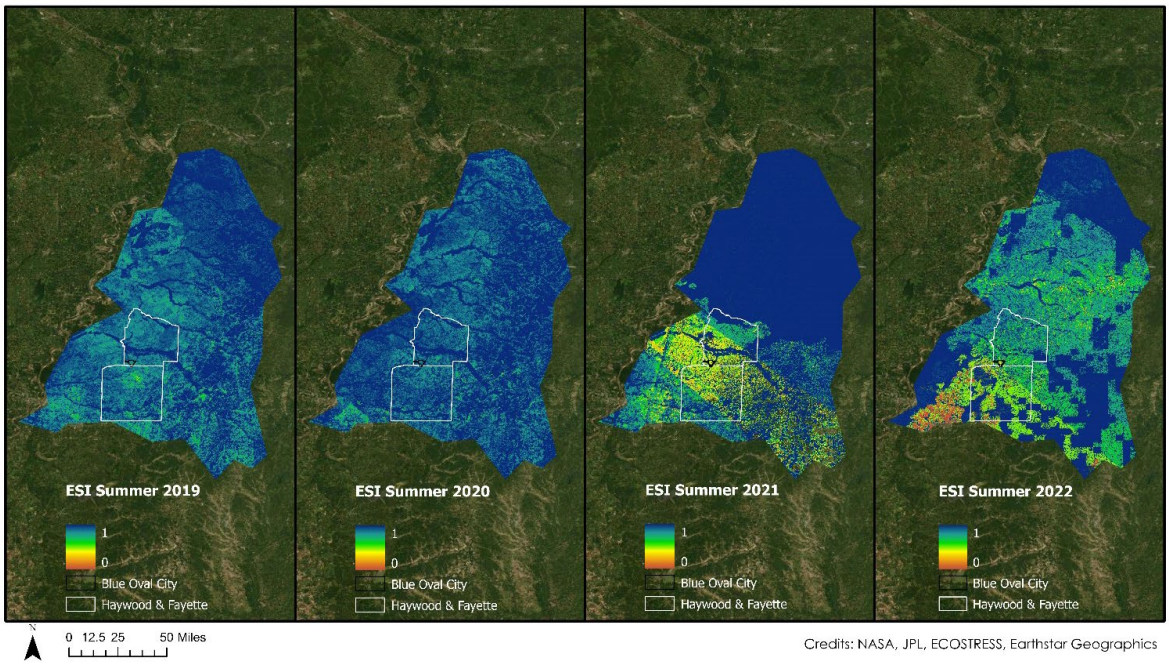

Figure C2 Summer Evaporative Stress Index

Appendix D

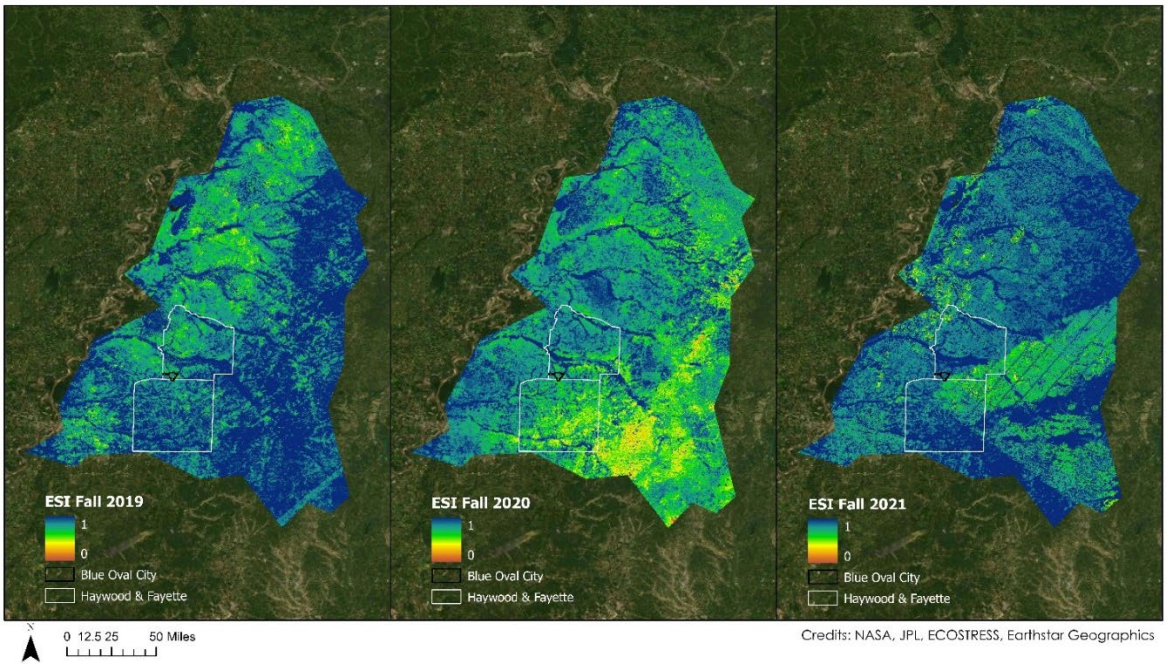

Figure D1 Fall Evaporative Stress Index

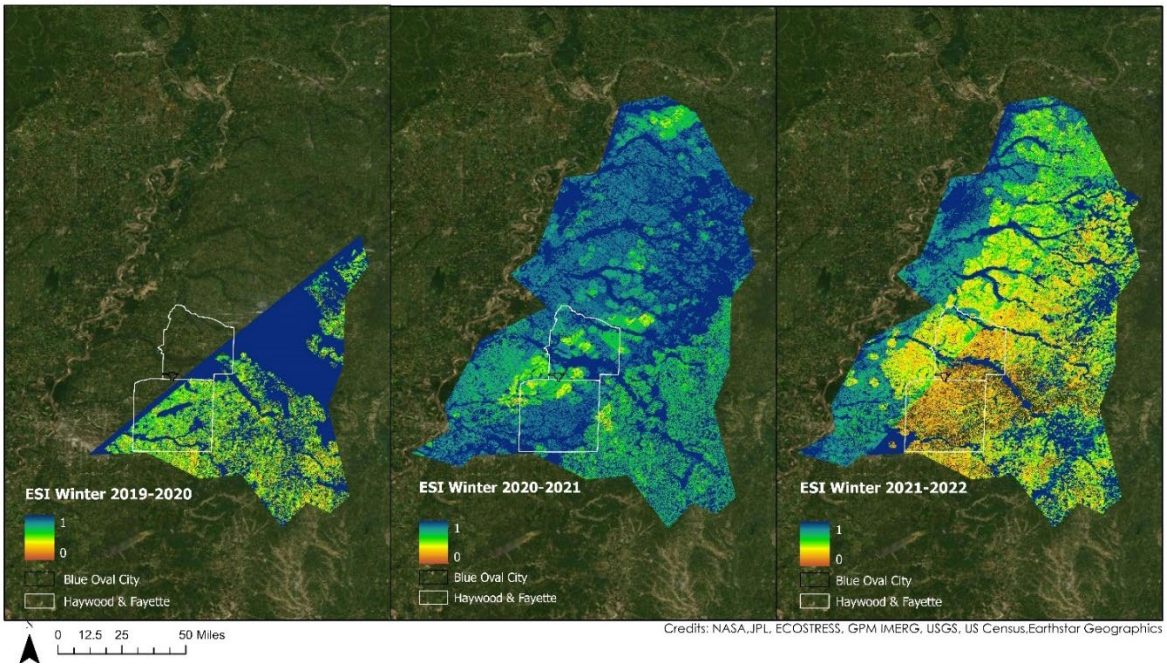

Figure D2 Winter Evaporative Stress Index

Appendix E

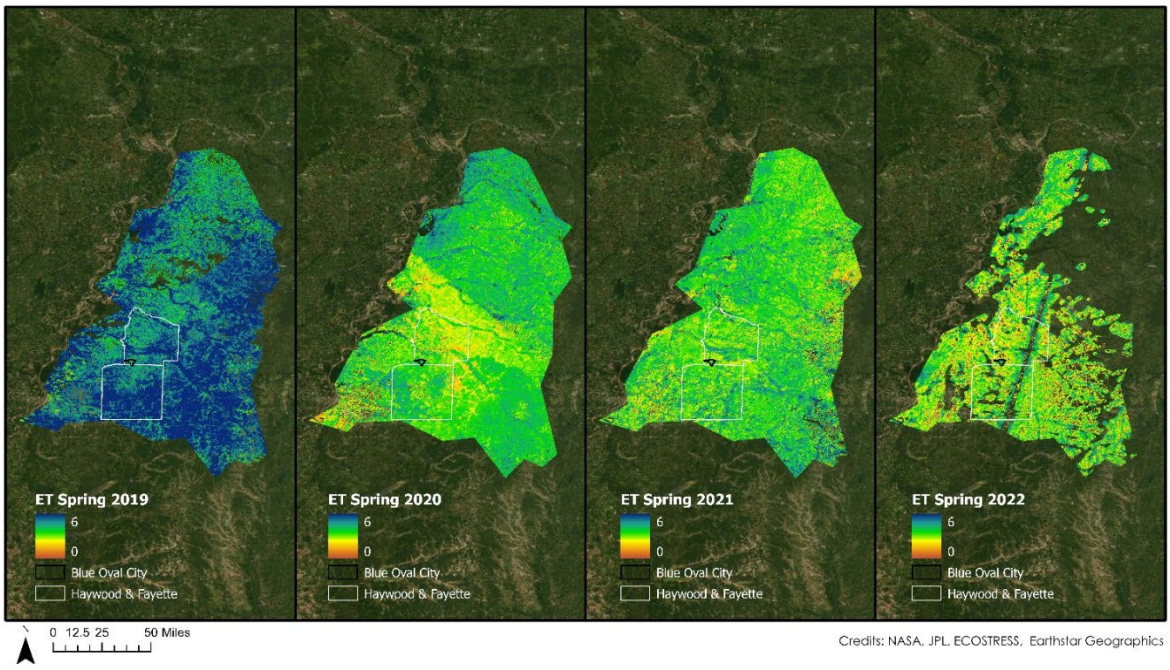

Figure E1 Spring Evapotranspiration

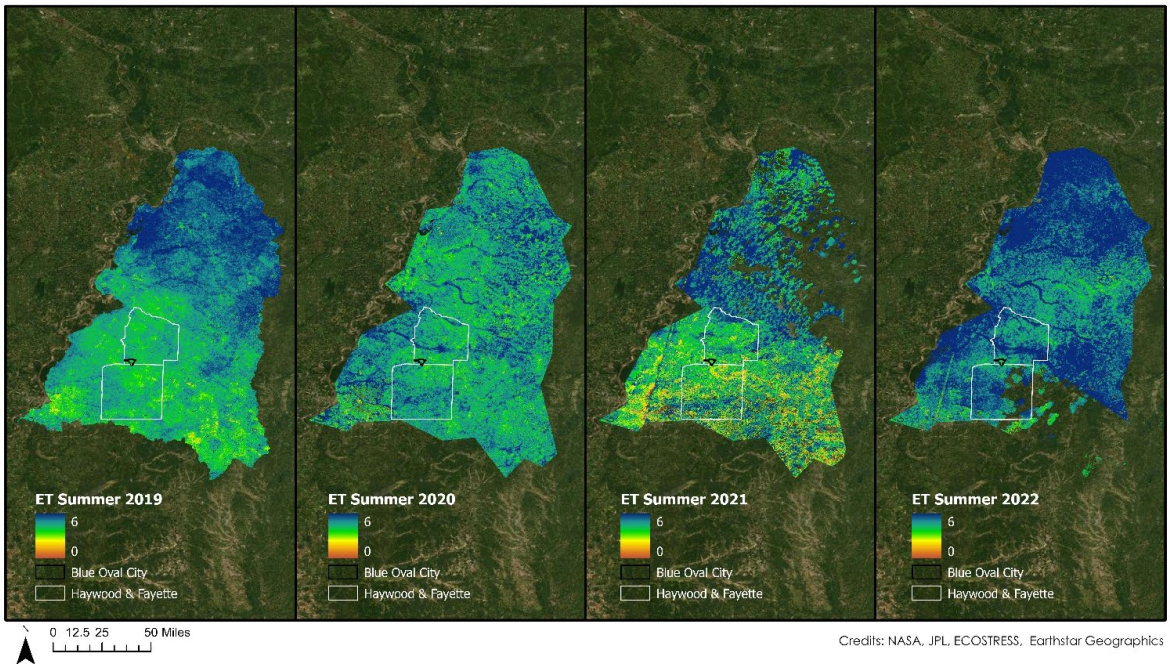

Figure E2 Summer Evapotranspiration

Appendix F

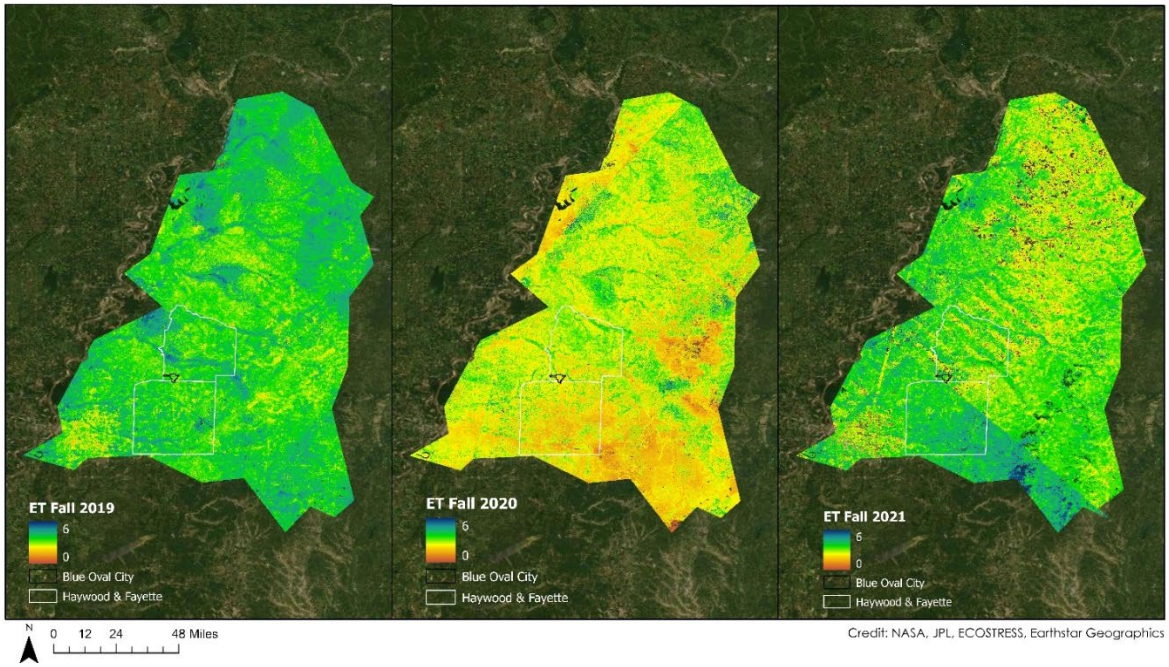

Figure F1 Fall Evapotranspiration

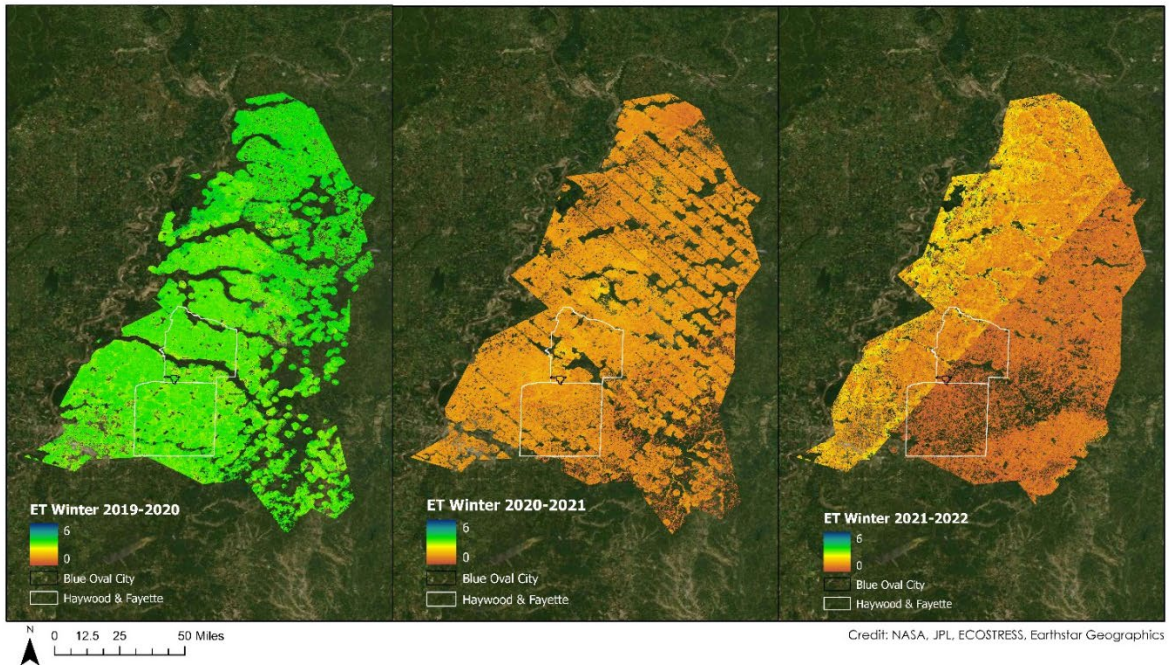

Figure F2 Winter Evapotranspiration

Appendix G

Table G1 Land cover classes

Remapped Value	NLCD 2019 Bands
0 – No data or Difficult to define pervious or impervious	31
1 - Trees	41, 42,43
2 - Pervious	21, 51,52, 71, 73, 74, 81, 82
3 - Developed	22, 23, 24
4 – Water	11, 12, 91, 95